Finite Element Analysis and Natural Frequency Optimization of Tapered Beam Using Glass Fiber Reinforced Plastic (GFRP)

[A]Surabhi Nikale

[A] Department of Mechanical Engineering, DY Patil College of Engineering
Savitribai Phule Pune University, Pune

Abstract- *Beams are very common types of structural components and it can be classified according to their geometric configuration as uniform or taper and slender or thick. If practically analyzed, the non-uniform beams provide a better distribution of mass and strength than uniform beams and can meet special functional requirements in architecture, aeronautics, robotics, and other innovative engineering applications. Design of such structures is important to resist dynamic forces, such as wind and earthquakes. It requires the basic knowledge of natural frequencies and mode shapes of those structures. The main of objectives of this project are to study and analyze vibration frequencies of conventional tapered beam designed as per design requirements and to design a composite tapered beam to replace conventional design and record its natural frequencies. After analysis of steel tapered beam and GFRP, the best angled lay-up tapered beam design from the different options of GFRP designs selected as per FEA modal analysis results will be manufactured. After manufacturing FFT Analyzer test for free vibration for manufactured final design of the GFRP tapered beam will be done. Then the results from FFT analyzer test results with the results of FEA analysis will be compared. From this project, we will be able to predict the best suited material for manufacturing the tapered beam as per vibration standards. We will be able to predict the best suited lay-up angles of GFRP tapered beam as per vibration standards.*

Key Words- GFRP, Layup angles, Analysis, FEA, Optimization

1. INTRODUCTION

1.1 Glass fiber reinforced polymer :

Glass is the most common material for fiber used in polymer matrix composites. The main types of glass are E-glass (also called "fiberglass") and S-glass. The "E" in the word E-glass stands for electrical as it was designed for electrical applications. However, E-glass is used for many other purposes now, like decorations and structural applications. The "S" in the word S-glass stands for higher content of silica. S-glass retains its strength at high temperatures compared to E-glass and has higher fatigue strength. It is used mainly for aerospace applications.Other types of glass available commercially are C-glass ("C" stands for corrosion) which is used in chemical environments, for example storage tanks; R-glass used in the structural applications such as buildings and construction; D-glass (dielectric) is used for applications requiring low dielectric constants, such as radomes; and A-glass (appearance) is used to improve surface appearance.

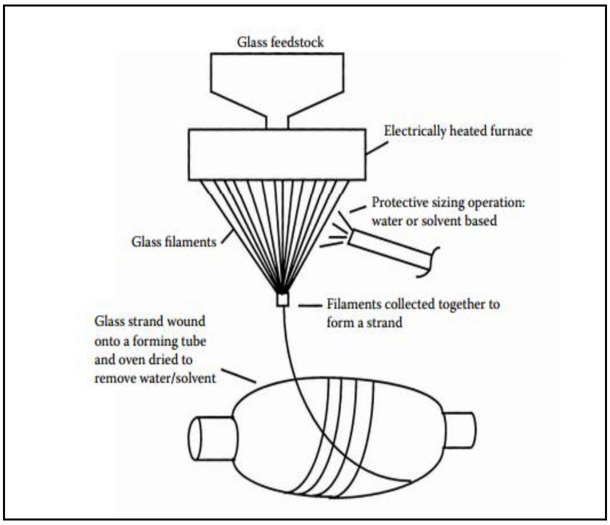

Fig. 1: Preparing Glass Strand

1.2 Fabrication of composite parts :

1. Hand lay-up

This technique is the simplest method of composite processing. The infrastructural requirement for this method is also minimal. The processing steps are quite simple. Firstly, a release gel is sprayed on the mould surface to avoid the sticking of polymer to the surface. Thin plastic sheets are used at the top and bottom of the mould plate to get good surface finish of the product. Reinforcement in the form of woven clothes or chopped strand mats are cut as per the mould size and placed at the surface of mould after Perspex sheet. Then thermosetting polymer in liquid form is mixed thoroughly in suitable proportion with a prescribed hardener (curing agent) and poured onto the surface of mat already placed in the mould. The polymer/resin is uniformly spread with the help of brush. Second layer of mat is then placed on the polymer surface and a roller is moved with a mild pressure on the mat- polymer layer to remove any air trapped as well as the excess polymer present. This process is repeated for each and every layer of polymer and mat, till the required layers are stacked. After placing the plastic sheet, release gel is sprayed on the inner surface of the top mould plate which is then kept on the stacked layers and the pressure is applied. After curing either at room temperature or at some specific temperature, mould is opened and the developed composite part is taken out and further processed.

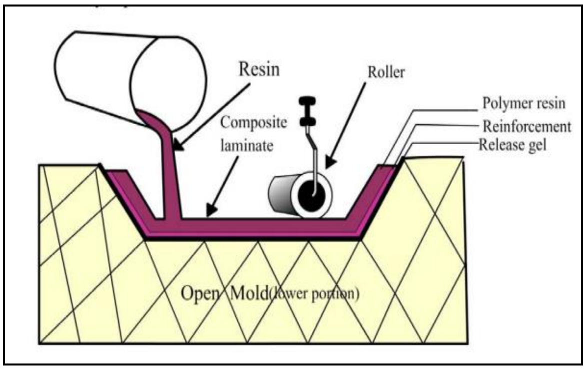

Fig. 2: Hand lay-up process of Composite Part Fabrication

1.3 Taguchi Method:

Orthogonal Arrays (often referred to Taguchi Methods) are often employed in industrial experiments to study the effect of several control factors. Popularized by G. Taguchi, other Taguchi contributions include:

- Model of the Engineering Design Process
- Robust Design Principle
- Efforts to push quality upstream into the engineering design process

An orthogonal array is one of the types of experiments where the columns for the independent variables are "orthogonal" to one another.

Benefits:

1. Conclusions valid over the entire region spanned by the control factors and their settings
2. Large saving in the experimental effort
3. Analysis is easy

To define an orthogonal array, one must identify:

1. Number of factors to be studied
2. Levels for each factor
3. Specific 2-factor interactions to be estimated
4. Difficulties that would be encountered in running the experiment

We know that with two-level full factorial experiments, we can estimate variable interactions. When two-level fractional factorial designs are used, we begin to confound our interactions, and often lose the ability to obtain unconfused estimates of main and interaction effects. We have also seen that if the generators are choosen carefully then knowledge of lower order interactions can be obtained under that assumption that higher order interactions are negligible.

Orthogonal arrays are highly fractionated factorial designs. The information they provide is a function of two things

- The nature of confounding
- Assumptions about the physical system.

2. LITERATURE SURVEY

Rajamohan Ganesan & Abolghassem Zabihollah presented a paper "Vibration analysis of tapered composite beams using a higher-order finite element" The objective of the present work is to conduct an investigation of the free undamped vibration response of such tapered composite beams, using the finite element method. Conventional cubic Hermitian finite element formulation requires a large number of elements to obtain reasonably accurate results in the analysis of tapered laminated beams. Since the continuity of curvature at element interfaces cannot be guaranteed with the use of conventional formulation, the stress distribution across the thickness is not continuous at element interfaces. The material and geometric discontinuities at ply drop-off locations leads to additional discontinuities in stress distributions. As a result, efficient and accurate calculation of natural frequencies becomes very difficult. In order to overcome these limitations, a higher-order finite element formulation is developed in Part I of the present work. The stiffness coefficients of the tapered laminated beam are determined based on the stress and strain transformations and classical laminate theory. In Part II of the present work, the developed formulation is used for the free undamped vibration analysis of various types of tapered composite beams and a parametric study is conducted.

R. Ghayoura, M. Ghayoura and S Ziaei-Rada presented a case on "Vibration analysis of tapered rotating composite beams using the hierarchical finite element" in which a hierarchical finite element model is presented for the flapwise bending vibration analysis of a tapered rotating multi-layered composite beam. The shear and rotary inertia effects are considered based on the higher shear deformation theory to derive the stiffness and mass matrices of a tapered-twisted rotating and composite beam element. Certain non-composite beams for which comparative results are available in the literature are used to illustrate the application of the proposed technique. Dimensionless parameters are identified from the equations of motion and the combined effects of the dimensionless parameters on the modal characteristics of the rotating composite beams are investigated through numerical studies. The results indicate that, compared with the conventionalities element method, the hierarchical finite element has the advantage of using fewer elements to obtain a better accuracy in the calculation of the vibration characteristics of rotating beams such as natural frequencies and mode shapes. Based on the proposed formulation, the mass and stiffness matrices of a tapered composite rotating beam element were developed for the eigenvalue analysis of rotating, doubly tapered beams. The element was found to give reasonably accurate results. The consideration of shear deformation was found to reduce the values of the higher natural frequencies of beam vibration. The results indicate that the hieratical finite element formulation uses fewer elements to obtain accurate results, which, in turn, leads to less costly computational processes. Comparison with available data reveals that the method is accurate and can be used for a large class of rotating beams. [2]

R. Vasudevan & B. Parthasaradhi In this study, free vibration responses of a rotating tapered composite beam with tip mass are investigated. The energy expressions for the kinetic and potential energies of a rotating composite beam with tip mass have been formulated. The energy expressions are then applied in Lagrange's equations to develop the equation of motion of a composite beam with tip mass. The stiffness and mass matrices for a standard composite beam element with two end nodes with two degrees of freedom at each node are derived. Various parametric studies are performed to investigate the effect of tip mass and the rotational speed on the variation of natural frequencies of the composite beam. The investigations are also done to study the effect of hub radius on the natural frequencies. It is shown that the addition of tip mass increases the stiffness of the structure and consequently increases the natural frequencies.[3]

Deepanshu Bhatt, Yogesh Mishra & Dr. P. K. Sharma presented a paper "Static and Free Vibration Analysis of Laminated Composite Plate by using Finite Element Method" in which Finite Element Method is used to solved Static and free vibration analysis. The Static analysis and free vibration analysis of orthotropic laminated composite plates are different materials are use. The ANSYS model is used to obtain the static and free vibration responses for laminated plates with different aspect ratios, thickness ratios and boundary condition under different support condition for different modes. In this work, a finite element model is being developed in ANSYS using APDL code. [4]

3. PROPOSED WORK

A. Objective of project

The objective of the work is:

1. Study and analyse vibration frequencies of conventional tapered beam designed as per design requirements.
2. Design a composite tapered beam to replace conventional design and record its natural frequencies.

B. Methodology

We have followed the following methodology in the course of the work completion

- To design tapered beam of steel and Aluminium Alloy using conventional design formulae
- To create 3 D model for steel and Aluminium Alloy tapered beam
- Perform Modal Analysis using FEA software to find out natural frequencies of the beams with different materials
- To design alternate tapered beam using GFRP material and create 3 D model for the same
- To create 3 D model for GFRP tapered beam
- To perform modal analysis on the GFRP tapered beams with different angle of orientations of lay ups for composite materials
- To manufacture the best angled lay-up tapered beam design from the different options of GFRP designs selected as per FEA modal analysis results
- To perform FFT Analyzer test for free vibration for manufactured final design of the GFRP tapered beam
- To compare the results from FFT analyzer test results with the results of FEA analysis

4. MATHEMATICAL CALCULATIONS

Design of tapered beam:

We have selected the wind pump blade as the application fr the tapered beam. From the design calculations we get the following parameters after designing the blade for steel material.

Table1: Design Specifications of Wind Mill

Rated Wind speed	3 m/s
Power Output	10.88 W
Windmill power required	60.77 W
Head of Water	12 m
Number of blade	18
Volume flow rate	8 m^3/day
Solidity	0.8
Rotor Diameter	2.2 m
Blade length	900 mm

4.1 Uniform Strength theory:

Consider it is a problem of Uniform Strength theory for varying width and constant thickness formula,

$$\sigma_{yt} = \frac{6\,F\,L}{B\,t^2}$$

L = blade length = 900 mm
B = min. width of blade = 110 mm
Take out blade material as GFRP with yield strength of 480 MPa, with factor of safety of 4,
So we get,

$$t2 = \frac{6\,F\,L}{\sigma_{yt}\,B}$$

$$= \frac{6 \times 18.44 \times 900}{110 \times {}^{480}/_{4}}$$

= 7.54
t = 2.75 mm
$t \cong 3\ mm.$
This is a blade thickness for wind mill pump.

Table 2: Final Design Specifications of GFRP Wind Pump Blade

Rated Wind speed	3 m/s
Power Output	10.88 W
Windmill power required	60.77 W
Head of Water	12 m
Number of blade	18
Volume flow rate	8 m^3/day
Solidity	0.8
Rotor Diameter	2.2 m
Blade length	900 mm
Blade Thickness	3mm

5. MODELLING AND ANALYSIS

The tapered beam to be optimized is shown below.

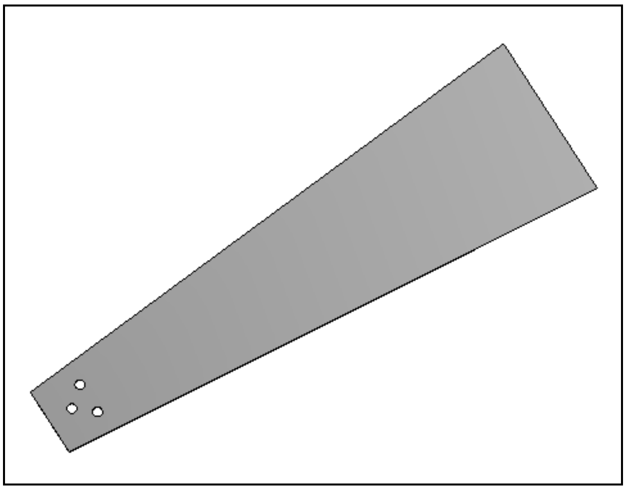

Fig. 3: Model of Steel Tapered Beam (Windmill Pump Blade)

5.1 FEA Results Steel Blade

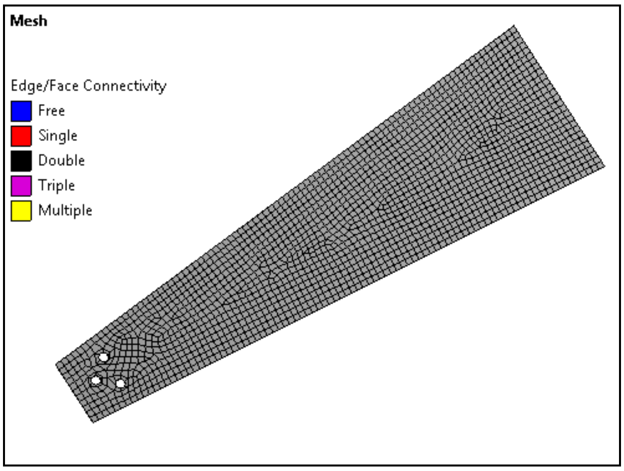

Fig. 4: Meshed Model of Steel Tapered Beam (Windmill Pump Blade)

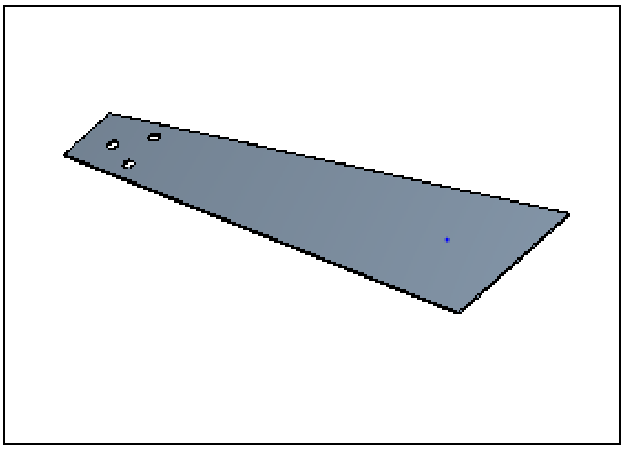

Fig. 5: Free Free Boundary condition

No boundary condition is applied to the bolt holes of the blade.

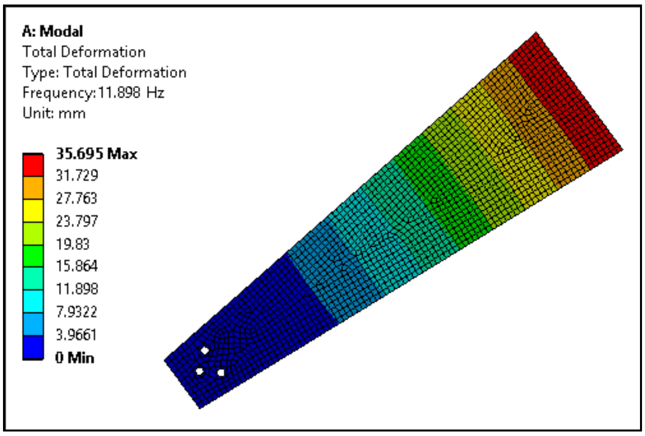

Fig. 6: Total Deformation plot for 1st mode shape of steel beam

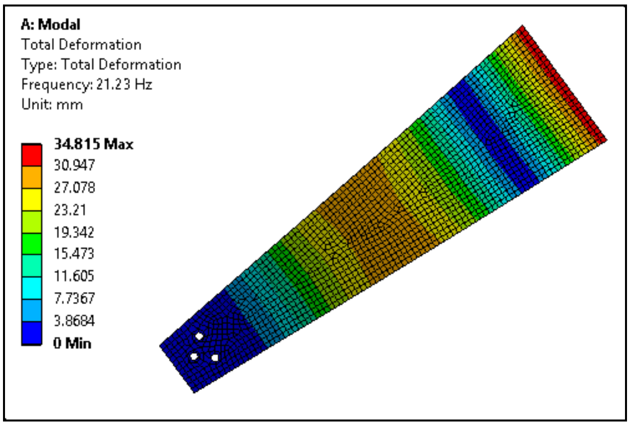

Fig. 7: Total Deformation plot for 2nd mode shape of steel beam

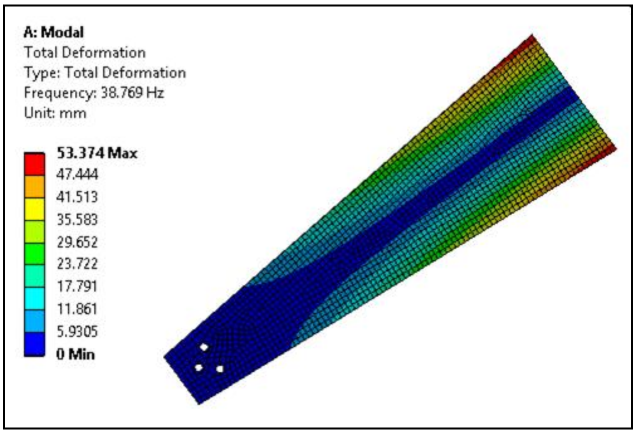

Fig. 8: Total Deformation plot for 3rd mode shape of steel beam

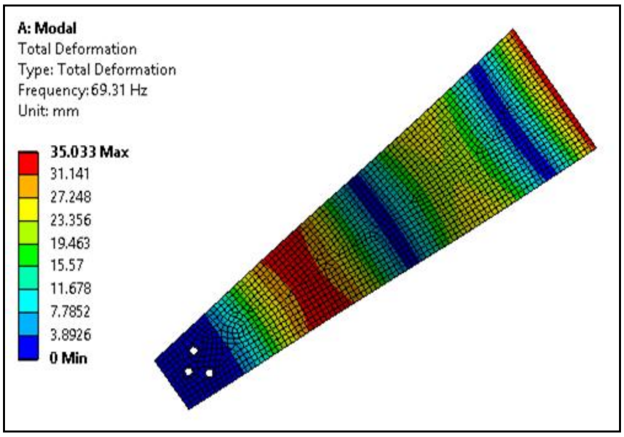

Fig. 9: Total Deformation plot for 4th mode shape of steel beam

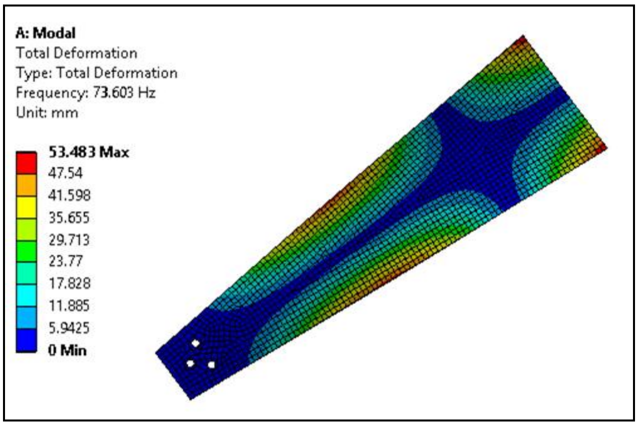

Fig. 10: Total Deformation plot for 5th mode shape of steel beam

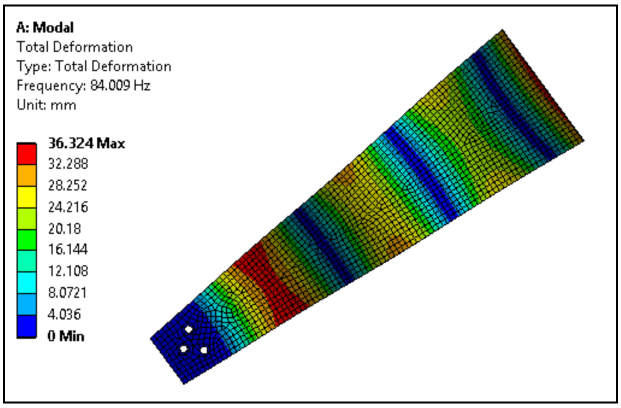

Fig. 11: Total Deformation plot for 6th mode shape of steel beam

From the FEA results obtained, we get the natural frequencies of the Steel Tapered Beam as shown in the below table:

Table 3:- Natural frequencies for steel tapered beam

Mode Shape	Natural Frequency
1	11.898
2	21.23
3	38.769
4	69.31
5	73.603
6	84.009

5.2 FEA Results GFRP Blades

Similarly as steel model, meshing and boundary condition images for GFRP blade are given below

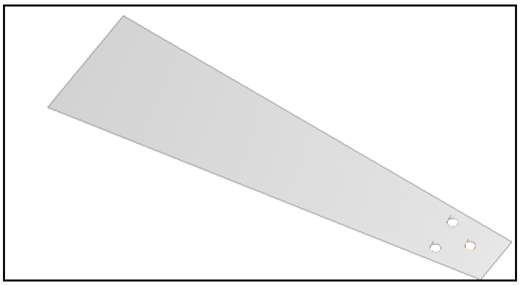

Fig. 12: Model for GFRP blade

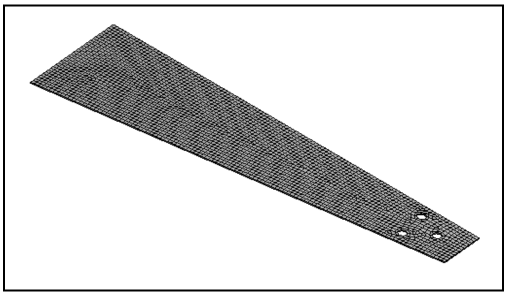

Fig. 13: Meshing for GFRP blade geometry

Shell 181 element type used for the meshing and 3000 nodes and 3000 elements are used for meshing the body.

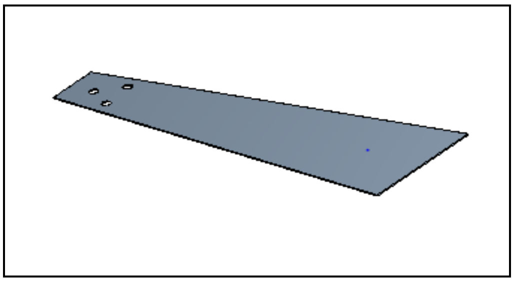

Fig. 14: Free Free Boundary condition

Thickness of the GFRP blade was calculated as 3 mm in design chapter using design calculations but there are different orientations of the ply angle that can be assigned to cloth we are using which will vary from 0 to 90 degrees. So permutations and combinations for the lay ups for different layers of cloth are formulated using taguchi matrix method. Results from the taguchi matrix analysis are given in the table of layer wise layup angle distribution in Taguchi Matrix section. By following those 9 combinations 9 runs will be performed on the FEA analysis of ANSYS. Results for all those experiments are given below.

e**xperiment1 (0-90,0-90,0-90)**

Material properties and ply setting used in the ANSYS Advance Composite module is shown in the image below.

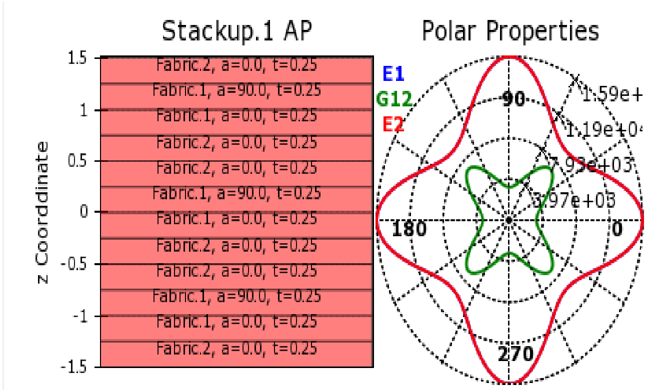

Fig. 15: Properties of the GFRP plies 0-90 glass fiber as fabric 1 with fabric 2 as resin epoxy

Figure shows that alternate layers of epoxy resin are applied on the Glass fiber woven cloth. Angle of the cloth is such that fiber orientations are kept 0-90 in all three layers of the cloth. Results for mode shapes and frequencies for this experiment are given below.

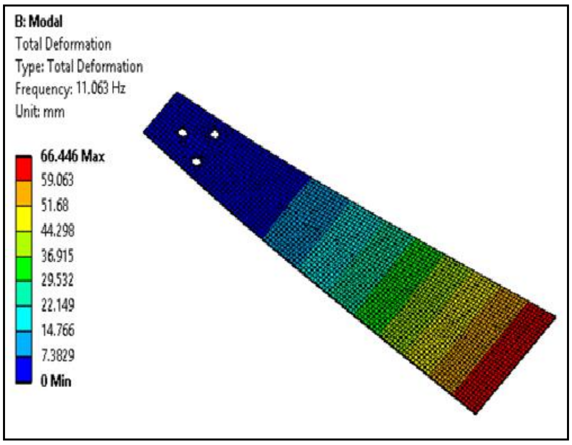

Fig. 16:- Mode shape plot 1 frequency 11.063 Hz

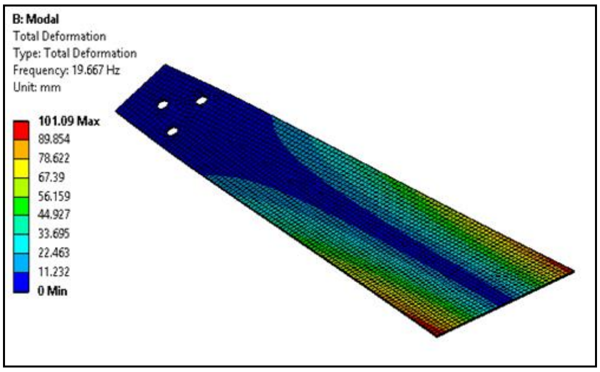

Fig. 17:- Mode shape plot 2 frequency 19.67 Hz

Table 4: – Modal frequency Summary Experiment 1

Mode Shape	Natural Frequency
1	11.063
2	19.667
3	38.02
4	66.52
5	69.64
6	86.09

experiment2 (0-90,45- -45,45- -45)

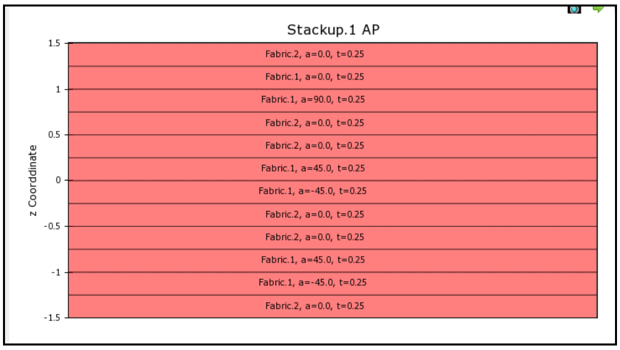

Fig. 18:- Stack up layer combinations Experiment 2 GFRP

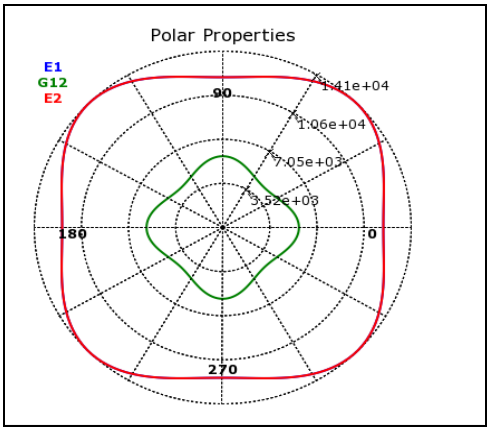

Fig. 19:- Polar properties of GFRP material

Figure shows that alternate layers of epoxy resin are applied on the Glass fiber woven cloth. Angle of the cloth is such that fiber orientations are kept 0-90 in first layer of the cloth and 45,-45 in the other two layers of the cloth. Results for mode shapes and frequencies for this experiment are given below.

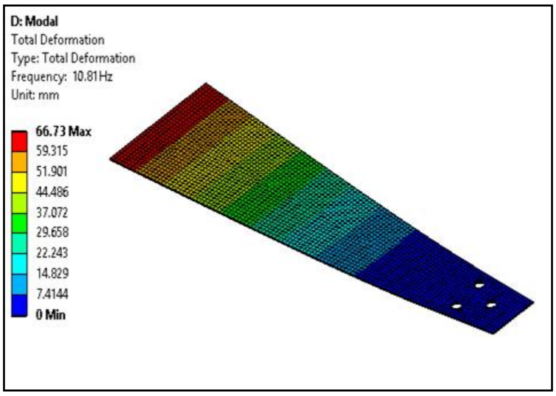

Fig. 20:- Mode shape plot 1 at frequency 1.8 Hz

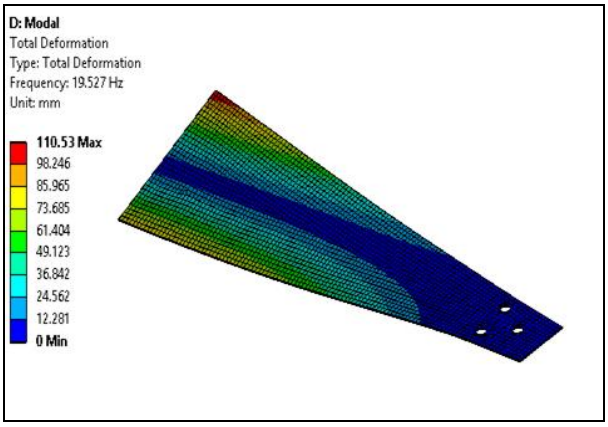

Fig. 21:- Mode shape plot 2 frequency 12.53 Hz

Table 5: – Modal frequency Summary Experiment 2

Mode Shape	Natural Frequency
1	10.81
2	19.527
3	37.89
4	66.36
5	68.93
6	88.23

experiment 3 (0,90 30,60 30,60)

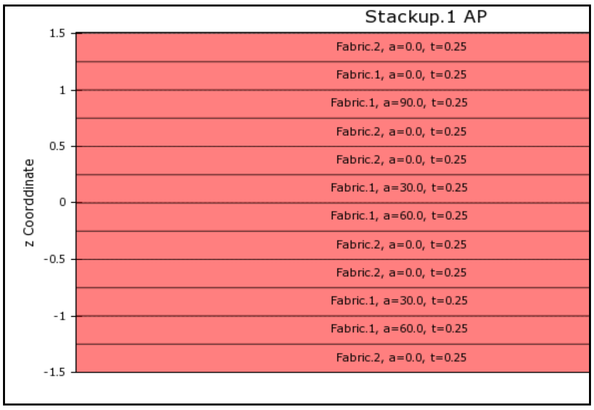

Fig. 22:- Stack up layer combinations Experiment 3 GFRP

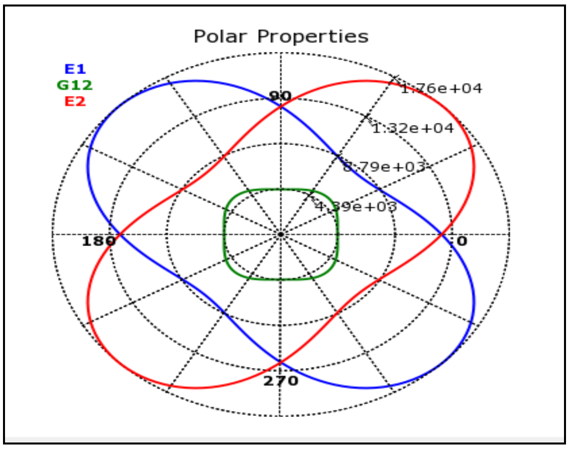

Fig. 23:- Polar properties of GFRP material Experiment 3

Figure shows that alternate layers of epoxy resin are applied on the Glass fiber woven cloth. Angle of the cloth is such that fiber orientations are kept 0-90 in first layer of the cloth and 30,60 in the other two layers of the cloth. Results for mode shapes and frequencies for this experiment are given below.

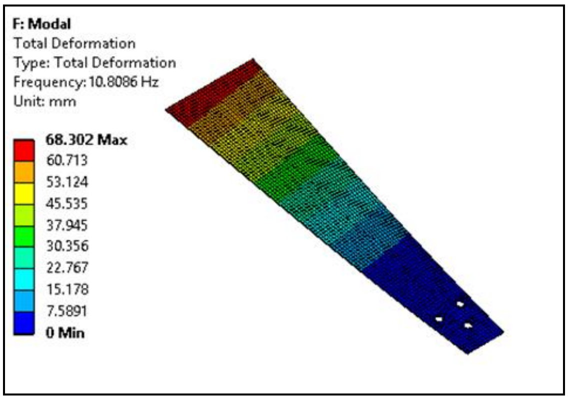

Fig. 24:- Mode shape plot 1 at frequency 10.80 Hz

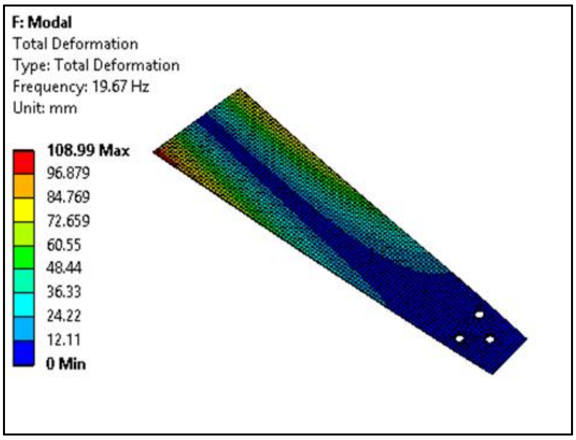

Fig. 25:- Mode shape plot 2 frequency 19.67 Hz

Table 6: – Modal frequency Summary Experiment 3

Mode Shape	Natural Frequency
1	10.8086
2	19.67
3	37.96
4	66.44
5	69.38
6	87.89

experiment 4 (45,-45 0,90 45,-45)

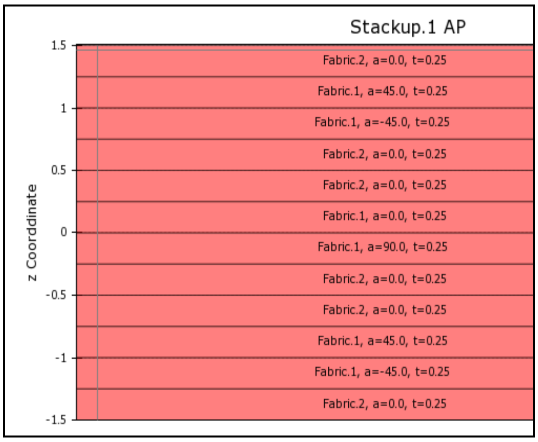

Fig. 26:- Stack up layer combinations Experiment 4 GFRP

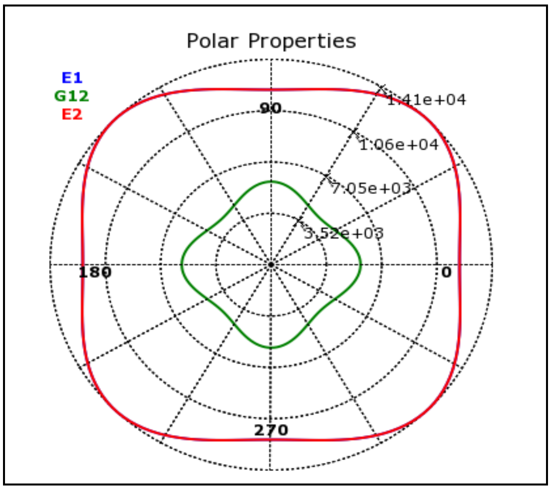

Fig. 27:- Polar properties of GFRP material Experiment 4

Figure shows that alternate layers of epoxy resin are applied on the Glass fiber woven cloth. Angle of the cloth is such that fiber orientations are kept 45,-45 in first and last layer of the cloth and 0, 90 in the middle layer. Results for mode shapes and frequencies for this experiment are given below.

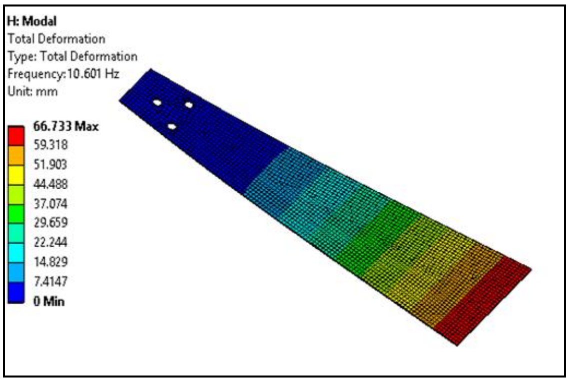

Fig. 28:- Mode shape plot 1 at frequency 10.60 Hz

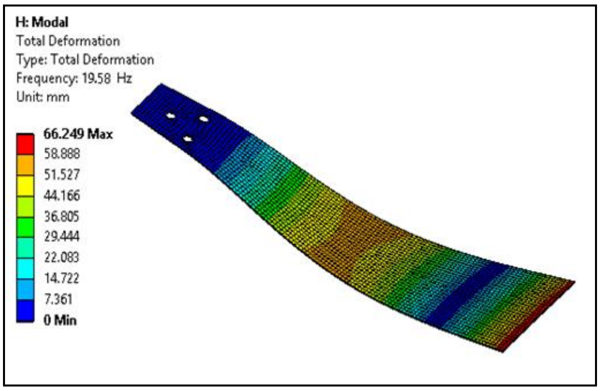

Fig. 29: - Mode shape plot 2 frequency 19.58 Hz

Table 7: – Modal frequency Summary Experiment 4

Mode Shape	Natural Frequency
1	10.601
2	19.58
3	37.84
4	66.32
5	68.84
6	87.74

experiment 5 (45,-45 45,-45 30,-60)

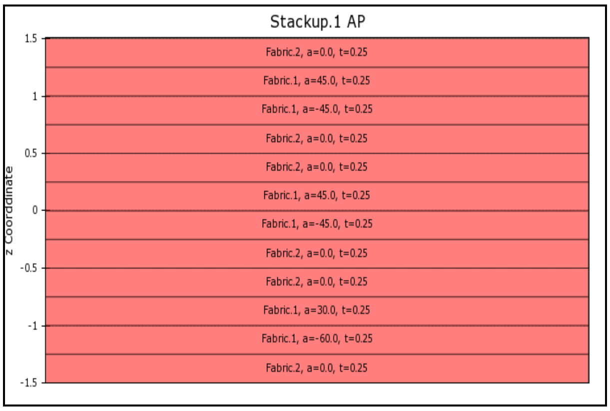

Fig. 30:- Stack up layer combinations Experiment 5 GFRP

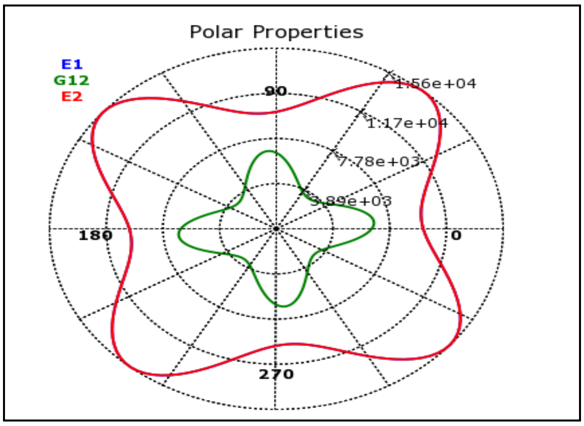

Fig. 31:- Polar properties of GFRP material Experiment 5

Figure shows that alternate layers of epoxy resin are applied on the Glass fiber woven cloth. Angle of the cloth is such that fiber orientations are kept 45,-45 in first two layers of the cloth and 30,-60 in the last layer. Results for mode shapes and frequencies for this experiment are given below.

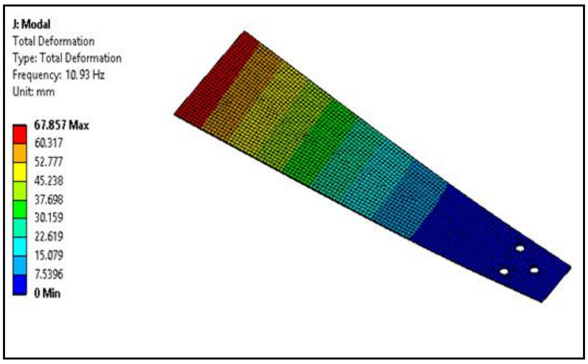

Fig. 32:- Mode shape plot 1 at frequency 10.93 Hz

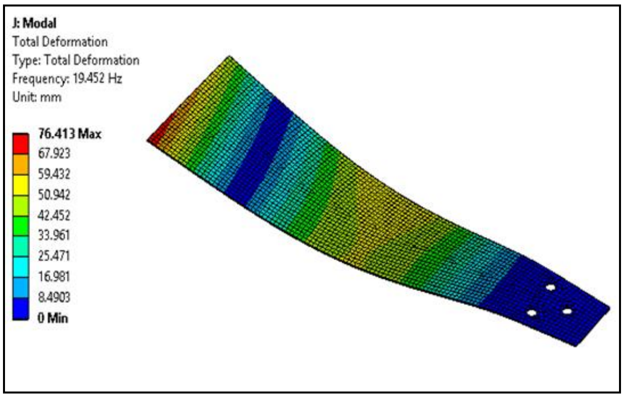

Fig. 33: - Mode shape plot 2 frequency 19.45 Hz

Table 8: – Modal frequency Summary Experiment 5

Mode Shape	Natural Frequency
1	10.93
2	19.452
3	38.36
4	66.48
5	69.59
6	88.23

experiment 6 (45,-45 30,-60 0,90)

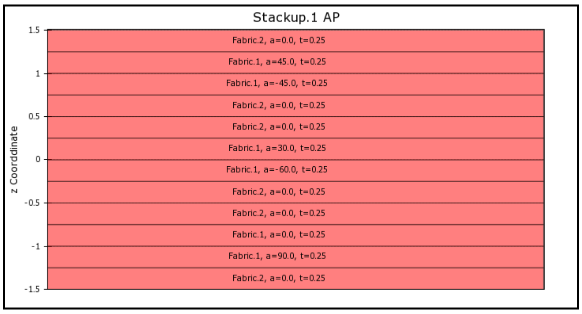

Fig. 34:- Stack up layer combinations Experiment 6 GFRP

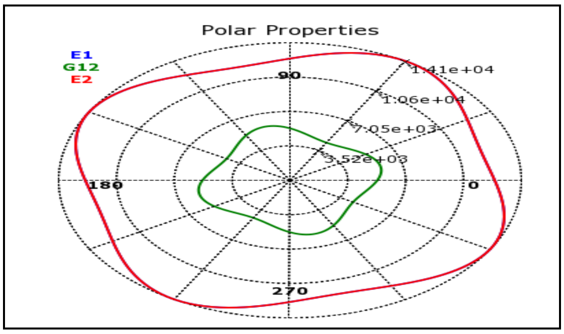

Fig. 35:- Polar properties of GFRP material Experiment 6

Figure shows that alternate layers of epoxy resin are applied on the Glass fiber woven cloth. Angle of the cloth is such that fiber orientations are kept 45,-45 in first layers, 30,-60 on the second layer and final layer of the cloth 0,90. Results for mode shapes and frequencies for this experiment are given below.

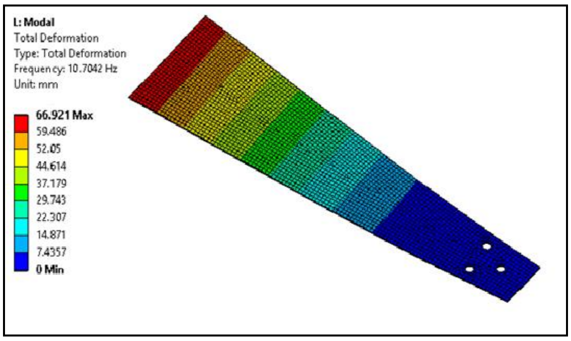

Fig. 36:- Mode shape plot 1 at frequency 10.70 Hz

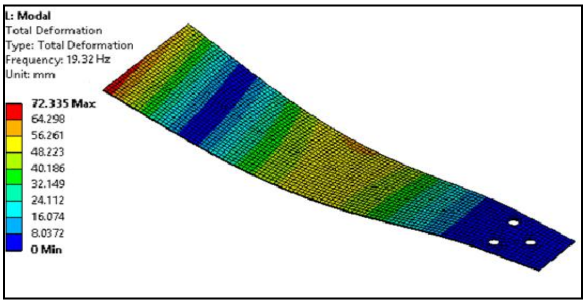

Fig. 37: - Mode shape plot 2 frequency 19.32 Hz

Table 9:– Modal frequency Summary Experiment 6

Mode Shape	Natural Frequency
1	10.7042
2	19.32
3	38.22
4	66.56
5	68.96
6	87.49

experiment 7 (30,-60 0,90 30,-60)

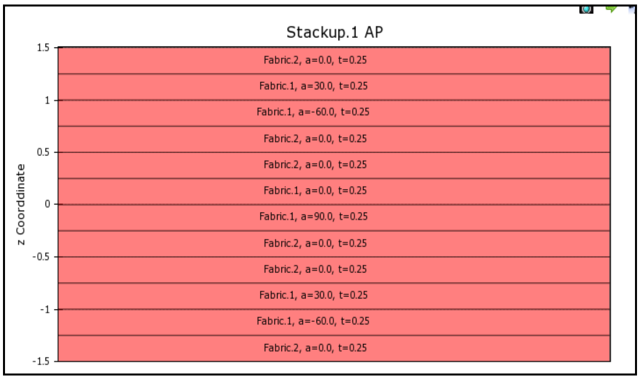

Fig. 38:- Stack up layer combinations Experiment 7 GFRP

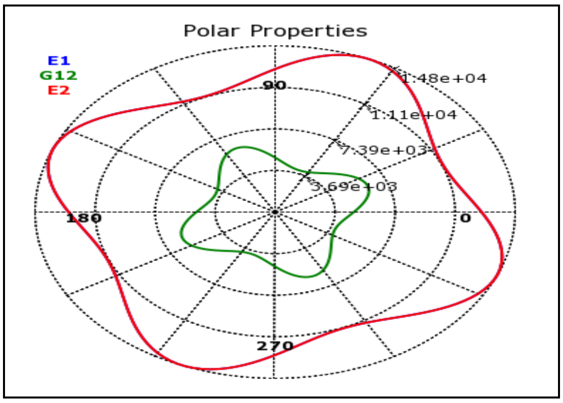

Fig. 39:- Polar properties of GFRP material Experiment 7

Figure shows that alternate layers of epoxy resin are applied on the Glass fiber woven cloth. Angle of the cloth is such that fiber orientations are kept 30,-60 in first and last layers, 0, 90 on the second layer. Results for mode shapes and frequencies for this experiment are given below.

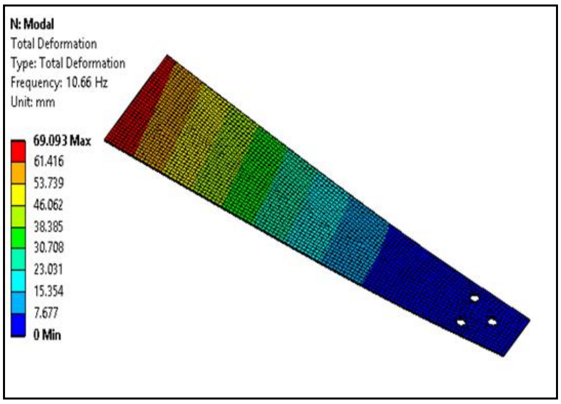

Fig. 40:- Mode shape plot 1 at frequency 10.66 Hz

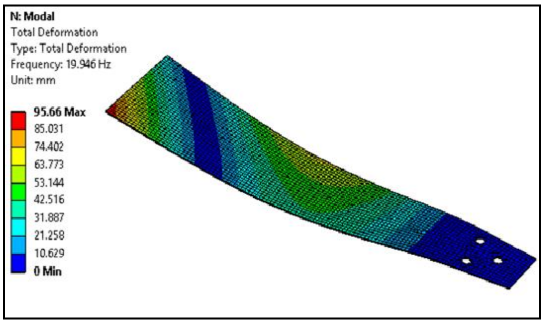

Fig. 41: - Mode shape plot 2 frequency 19.95 Hz

Table 10:– Modal frequency Summary Experiment 7

Mode Shape	Natural Frequency
1	10.66
2	19.946
3	37.84
4	65.96
5	69.43
6	87.34

experiment 8 (30,-60 45,-45 0,90)

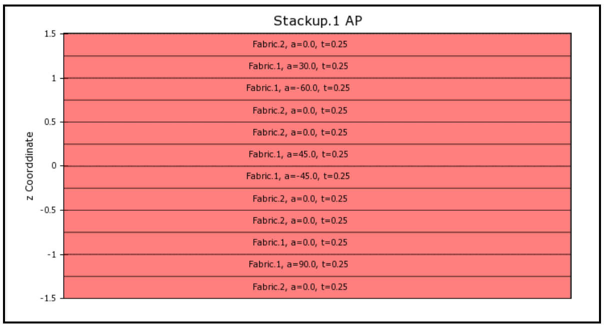

Fig. 42:- Stack up layer combinations Experiment 8 GFRP

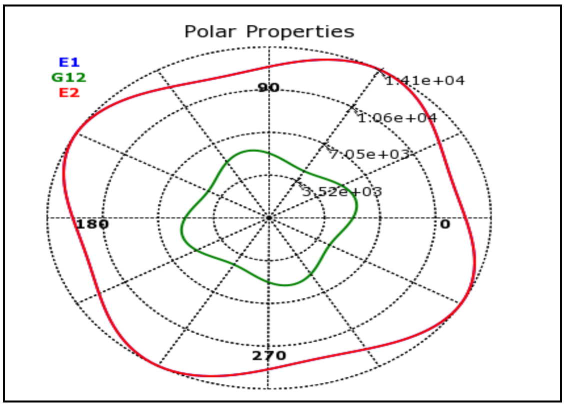

Fig. 43:- Polar properties of GFRP material Experiment 8

Figure shows that alternate layers of epoxy resin are applied on the Glass fiber woven cloth. Angle of the cloth is such that fiber orientations are kept 30,-60 in first layer, 45,-45 in the second layer and last layers is of 0,90. Results for mode shapes and frequencies for this experiment are given below.

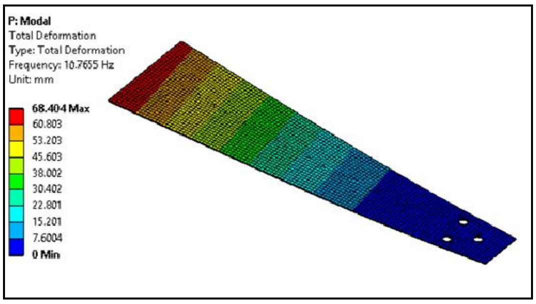

Fig. 44:- Mode shape plot 1 at frequency 10.76 Hz

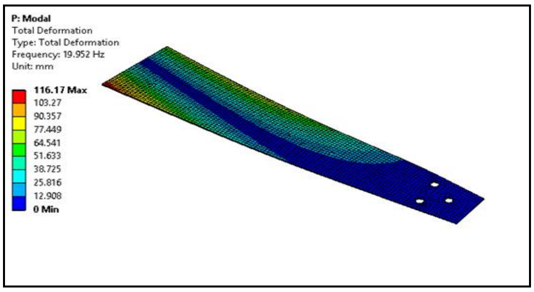

Fig. 45: - Mode shape plot 2 frequency 19.95 Hz

Table 11:– Modal frequency Summary Experiment 8

Mode Shape	Natural Frequency
1	10.76
2	19.952
3	38.59
4	65.68
5	69.32
6	87.33

experiment 9 (30,-60 30,-60 45,-45)

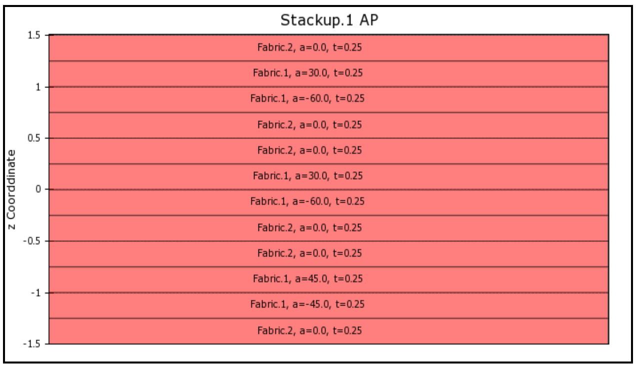

Fig. 46:- Stack up layer combinations Experiment 9 GFRP

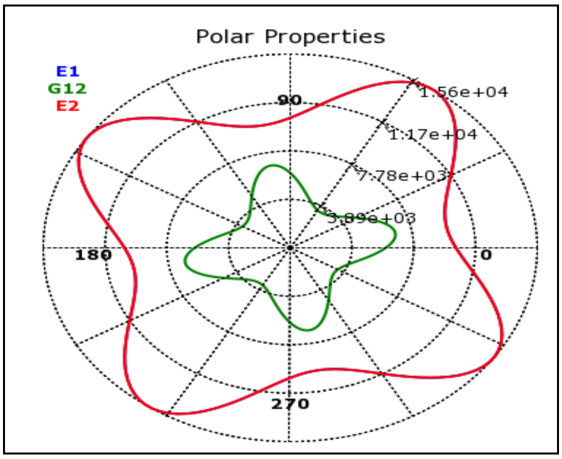

Fig. 47:- Polar properties of GFRP material Experiment 9

Figure shows that alternate layers of epoxy resin are applied on the Glass fiber woven cloth. Angle of the cloth is such that fiber orientations are kept 30,-60 in first two layers, 45,-45 in the last layer. Results for mode shapes and frequencies for this experiment are given below.

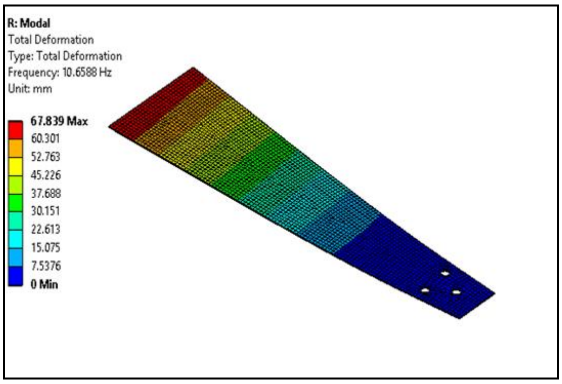

Fig. 48:- Mode shape plot 1 at frequency 10.65 Hz

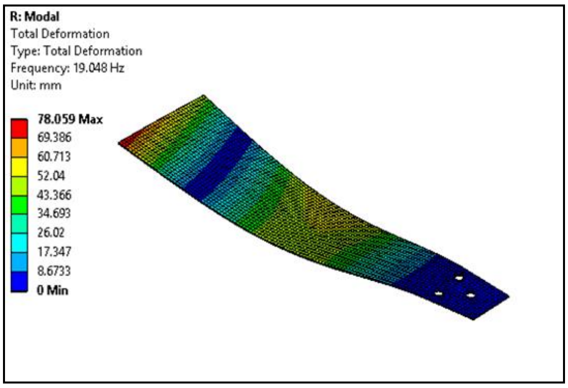

Fig. 49: - Mode shape plot 2 frequency 19.05 Hz

Table 12:– Modal frequency Summary Experiment 9

Mode Shape	Natural Frequency
1	10.65
2	19.048
3	38.49
4	66.37
5	68.54
6	88.23

Finite Element Analysis results for the all 9 experiments performed are to be compared to find out the best suitable combination to replace steel.

Table 13:- FEA summary

Material	Natural Frequency					
Mode Shape No	1	2	3	4	5	6
Steel	11.89	21.23	38.76	69.31	73.603	84.01
GFRP Exp. 1	11.06	19.66	38.02	66.52	69.64	86.09
GFRP Exp. 2	10.81	19.52	37.89	66.36	68.93	88.23
GFRP Exp. 3	10.80	19.67	37.96	66.44	69.38	87.89
GFRP Exp. 4	10.60	19.58	37.84	66.32	68.84	87.74
GFRP Exp. 5	10.93	19.45	38.36	66.48	69.59	88.23
GFRP Exp. 6	10.70	19.32	38.22	66.56	68.96	87.49
GFRP Exp. 7	10.66	19.94	37.84	65.96	69.43	87.34
GFRP Exp. 8	10.76	19.95	38.59	65.68	69.32	87.33
GFRP Exp. 9	10.65	19.04	38.49	66.37	68.54	88.23

It can be clearly seen that only experiment 1 has the first natural frequency as good as steel and all the other are lagging in the first natural frequency of the blade at the least by 9.72%. So it will be clear choice to choose first experiment combination as a replacement to the steel. As from the other natural frequencies of the first experiment are lagging from the steel , most important property in the dynamic frequency analysis is to find out and compare lowest natural frequency for the given free boundary condition and which is matching in the case of first experimental combination. So same should be manufactured and tested with FFT analyzer to compare frequencies with the analysis.

6. EXPERIMENTAL VALIDATION PLAN

PROCEDURE FOR DETERMINATION OF NATURAL FREQUENCIES IS AS FOLLOWS:

1) Select a peak value of vibration.
2) Check phase difference for that peak value, it is expected to be 180°. If this condition is satisfied then go for 3rd step and if not then select next pick and follow steps 1 and 2.
3) Check coherence for that corresponding pick, it is expected to be one ideally (0.75 to 1 can also be chosen). If this condition is satisfied then corresponding peak will give first natural frequency and if not then select next peak and follow steps 1, 2 and 3 again. In this way we can get First natural frequencies by using FFT analyzer.

The image of the FFT Testing is as shown below.

Fig. 50:-Experimental setup image 1

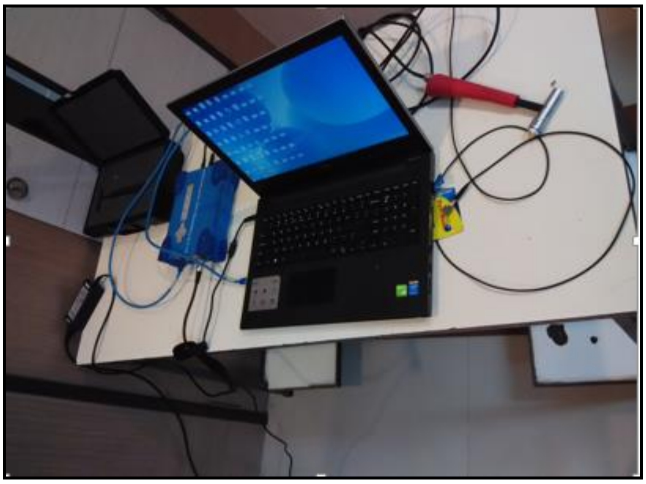

Fig. 51:-Experimental setup image 2

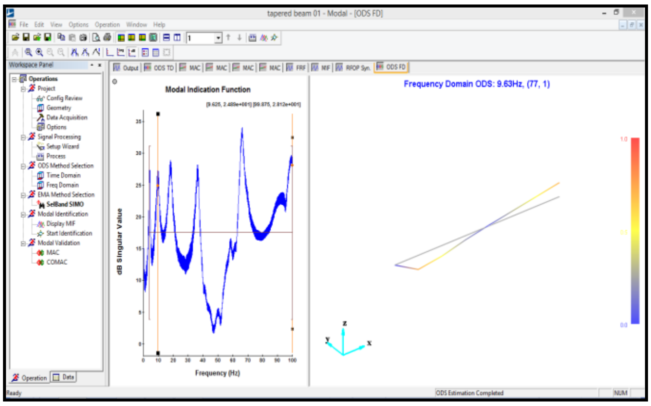

Fig. 52:-Experimental results

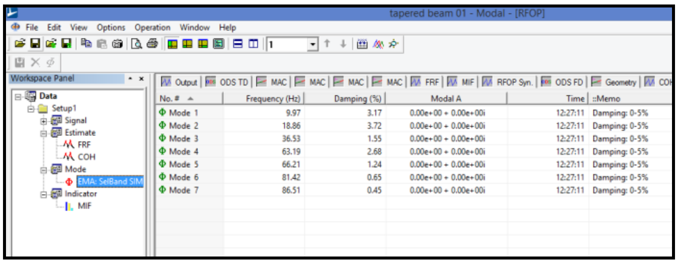

Fig. 53:-Experimental results of all mode shape

Material	Natural Frequency					
Mode Shape No	1	2	3	4	5	6
FFT	9.97	18.86	36.53	63.19	66.21	81.42

7. RESULTS AND DISCUSSION

It can be summarized from the FEA analysis chapter and taguchi matrix experimental results that first natural frequency observed as 11.063 Hz, for the experiment 1 which is combination of all 3 0-90 orientation layers. Which is the highest first natural frequency observed for the GFRP with combinational orientation of layup angles studied. Lowest first natural frequency was observed for the combinations in experiment 4 and 9 combinations which is around 10.6 Hz.

Mode shape plots observed for steel and GFRP with 0-90 layup angles are similar in nature. There is difference in the natural frequencies of the GFRP and steel when we go to the higher value of modes. As our study is based on finding the best first natural frequency for the GFRP combinations which should be replaceable in place of steel. Some graphs are plotted below against the experiment number performed.

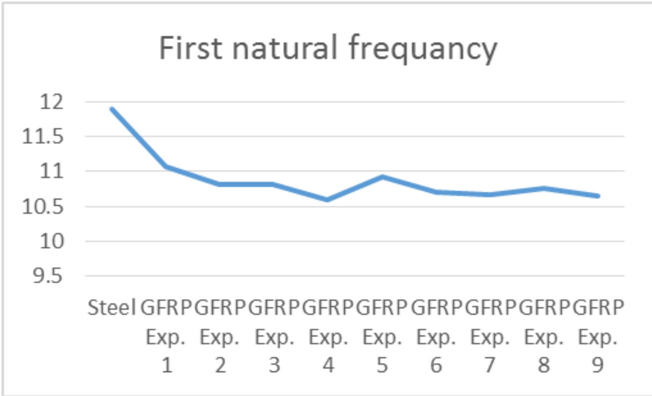

Fig. 54:- Graph of First natural frequency vs Blade model in FEA

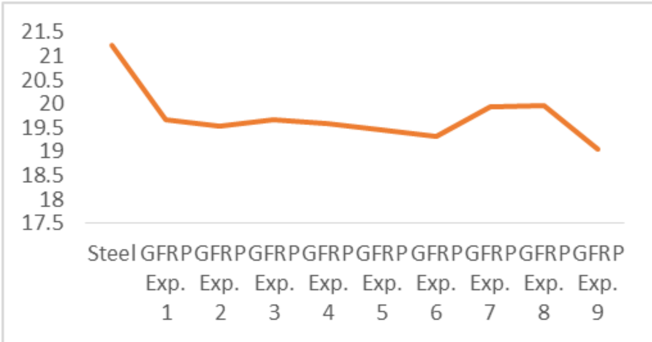

Fig. 55:- Graph of Second natural frequency Vs Blade model in FEA

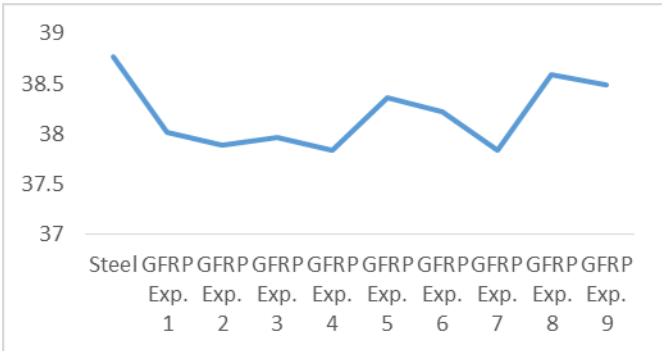

Fig. 56:- Graph of Third natural frequency Vs Blade model in FEA

	Natural Frequency					
Mode Shape No	1	2	3	4	5	6
Steel	11.898	21.23	38.769	69.31	73.603	84.01
GFRP Exp. 1	11.063	19.667	38.02	66.52	69.64	86.09
FFT Results	9.97	18.86	36.53	63.19	66.21	81.42

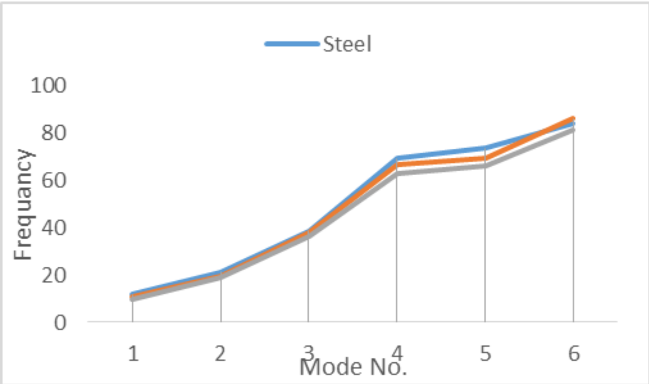

Fig. 57:- Graph of comparison of Steel, FEA and FFT results

CONCLUSION

- Steel and GFRP blade for the wind pump is successfully designed and simulated in FEA and results are within the acceptance criteria for both.
- It can be clearly concluded from the design and FEA chapter that conventional blade for the turbine can be replaced with the GFRP design by saving weight without affecting the structural performance in terms of material failure.
- From FEA analysis performed of taguchi matrix lay up combinations it can be safely concluded that cloth angle of 0-90 for all three layers will provide best results of the first modal natural frequency which is comparable with the steel.
- This mean modal frequency performance of the blade design is also not changing if we replace the steel blade with the 0-90 layup angled GFRP blade.
- GFRP blade successfully manufactured and tested for finding out modal frequencies.

REFERENCES

1. Vibration Analysis Of Tapered Beams Using A Higher Order Finite Element Analysis, Rajamohanan Ganesan and Abolghassem Zabihollah, Science Direct Composite Structures, doi 10.1016.

2. Vibration analysis of tapered rotating composite beams using the hierarchical finite element, by R. Ghayoura, M. Ghayoura, S. Ziaei-Rada, Applied and Computational Mechanics, 21 June 2010.

3. Vibration Analysis Of A Rotating Tapered Composite Beam With Tip Mass R.Vasudevan1 & B. Parthasaradhi ,International Journal of Mechanical and Industrial Engineering (IJMIE) ISSN No. 2231 –6477, Vol-2, Iss-3, 2012.

4. A Review of Static and Free Vibration Analysis of Laminated Composite Plate by using Finite Element Method Deepanshu Bhatt, Yogesh Mishra & Dr. P.K. Sharma International Journal of Advanced Engineering and Global Technology.

5. Boundary condition identification of tapered beam with flexible supports using static flexibility measurements Le Wang, Ning Guo & Zhichun Yang, ELSEVIER, Mech. Syst. Signal Process. (2016).

6. Finite element beam analysis of tapered thin-walled box beams Dongil Shin, Soomin Choi, Gang-Won Jang &Yoon Young Kim, ELSEVIER Thin-Walled Structures 102 (2016) 205–214.

7. Free vibration and wave propagation analysis of uniform and tapered rotating beams using Spectrally formulated finite elements K. G. Vinod, S.